A FULLY-INTEGRATED CMOS-MEMS AUDIO MICROPHONE

J. J. Neumann, Jr., and K. J. Gabriel
MEMS Laboratory, ECE Dept., 1209 Hamerschlag Hall, Carnegie Mellon University, 5000 Forbes Ave., Pittsburgh, PA
15213-3890, USA. Tel.: (412) 268-4404, Fax: (412) 268-4595, e-mail: jneumann@ece.cmu.edu

ABSTRACT

We report on the construction of a microphone and associated electronics fabricated entirely within a standard CMOS (complementary metal oxide semiconductor) die. An A-weighted noise level of 46 dB SPL was achieved with a total diaphragm area of 0.61mm^2. Because the microphone uses the same processing sequence as CMOS-MEMS (microelectromechanical systems) microspeakers [1], it is now possible to create acoustic systems-on-chip for applications in such areas as hearing aids, in-ear translators, and active noise cancellation. Because electret materials are not used, the microphone can withstand temperatures up to 250 °C with no degradation in performance. The frequency-modulated output provides a convenient, low-noise way to transmit the signal off chip, and is directly compatible with digital circuitry and FM radios.

INTRODUCTION

MEMS provides several advantages over conventional ways of building microphones. The most obvious are the economics of manufacturing mass quantities in the existing semiconductor fabrication and packaging infrastructure, and the possibility of including integrated electronics. The smaller size also allows new applications, such as surveillance and multiple transducers in a small area. In theory, the thinner diaphragms also permit better fundamental noise and sensitivity performance and vibration rejection for a given surface area than traditional microphones. Several approaches to MEMS microphones have already been taken. In one very similar to this work, additional layers (polyimide and metal) were deposited on a CMOS chip and micromachined [2]. Polysilicon [3] or silicon [4] may also be used to form the diaphragm. It is also possible, using thermal methods, to measure airflow directly in three dimensions, rather than pressure [5], which greatly simplifies sound intensity measurements.

In our work presented here, the traditional "condenser" or capacitive microphone approach is used, but integrated with CMOS electronics in a way that minimizes custom processing steps. This results in a technology which can be mass produced commercially, while maintaining design flexibility, taking advantage of advances in semiconductor fabrication as they occur in the industry at large.

TECHNOLOGICAL APPROACH

The microphone diaphragms are formed from the existing CMOS layers using a variant of the CMOS-based micromachining technique developed at Carnegie Mellon University [6,1]. A serpentine metal and oxide mesh pattern (0.9 μm-wide beams and gaps) is repeated within the diaphragm area, and the underlying silicon is etched out to form a suspended mesh membrane. A Teflon™-like conformal polymer (0.5-1.0 μm) is then deposited onto the chip, covering the mesh and creating an airtight seal over a cavity. Depending on the membrane geometry and gap between the membrane and substrate, a capacitance of 0.1 pF to 1 pF can be achieved. Vent holes are etched from the back, allowing greater movement of the diaphragm and providing a mechanism for controlled damping of resonant oscillations.

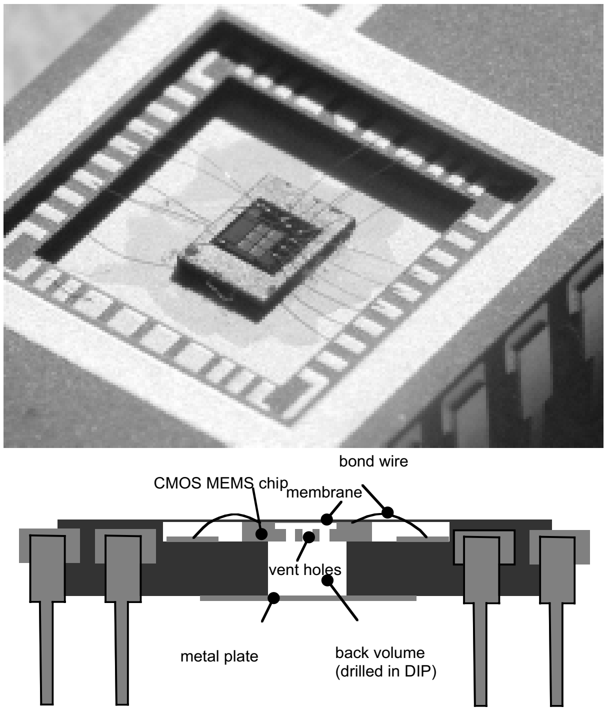

Figure 1: Photo and drawing showing the microphone chip mounted on a DIP package, with the vent holes positioned above the hole in the DIP package. This provides an acoustic back volume, and the metal plate isolates the back of the chip from the sound pressure field.

Sound impinges on an array of six 320 μm square sensing diaphragms, which act as electrodes of a capacitor, varying the frequency of the on-chip 100 MHz oscillator of which they are a part. The frequency modulation (FM) provides a convenient, low-noise way to transmit the signal off chip, and is directly compatible with digital circuitry and FM radios.

The CMOS-MEMS microphone chip is shown in Figure 1.

MODELS AND PARAMETERS

The transduction behavior may be predicted by considering the acoustic and the electrical behavior of the chip. Because the acoustic wavelengths of interest (>10 mm) are much greater than the dimensions of the microphone (< 2 mm), the acoustic behavior may be modeled by a lumped-parameter electrical equivalent circuit (Figure 2). In this analogy, the sound pressure p (deviation from ambient atmospheric pressure) is analogous to voltage in the electrical equivalent circuit, and the volume velocity U (volume of air moved per unit time) corresponds to electrical current. Thus, acoustic impedance is defined to be $Z=p/U$. Acoustic compliances are modeled as capacitors, air mass as inductance, and dissipative (frictional) effects as resistors [7].

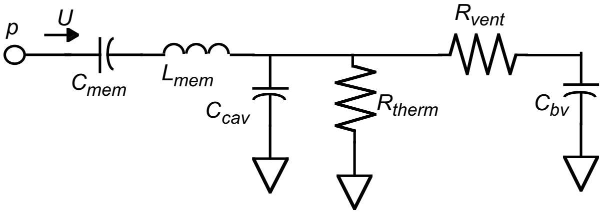

Figure 2: Electrical analog to acoustic behavior of microphone system.

The sound pressure impinges on the left terminal of the circuit. Because the device and packaging are both much smaller than acoustic wavelengths of interest, we may neglect the pressure-doubling effect caused by diffraction. Capacitor C_{mem} and inductor L_{mem} model the compliance and mass of the membrane, respectively. Material properties of the membrane derived in previous work [1] were used. We used an effective Young's modulus E = 800 MPa, and a density ρ = 1900 kg/m^3 for the mesh/polymer combination. C_{cav} is the compliance of the air in the gap between the membrane and the silicon substrate. This is modeled as a purely isothermal compression because of the strong heat conduction between the air in the gap and the silicon it contacts (large area/volume ratio). It can be shown that the dissipative part of the compression is negligible in the limits of pure adiabatic and pure isothermal compression, so we set R_{therm} to infinity. R_{vent} models the acoustic resistance due to the viscosity in the vent holes. C_{bv} is the compliance of the back volume, in our case several mm^3 drilled in the DIP package. This compression is approximately adiabatic because of the larger volume. Its impedance is also the major limitation on sensitivity along with the impedance of the membrane.

For a given sound pressure p, the change in capacitance may be calculated by finding the volume velocity U and deriving the membrane displacement. From this, the modulation amount of the oscillator may be calculated as a function of sound pressure. The predicted response is shown together with the measured response in the results section.

EXPERIMENTAL PROCEDURE

Figure 3 shows the setup used for the microphone measurements. The sensitivity of the Bruel and Kjaer (B&K) 4939 reference microphone is known, and was used to measure the sound pressure level (SPL) inside the anechoic box (B&K 4232). The reference microphone and the MEMS device under test were placed in symmetrical positions relative to the speaker's axis. The reference microphone signal was fed through a B&K 2669 preamp and B&K 2690 Nexus conditioning amp. The electrical output of the MEMS device was connected to the antenna input of the stereo receiver (Pioneer SX-303R) through a 3.2 Kohm resistor and 150 pF capacitor in series.

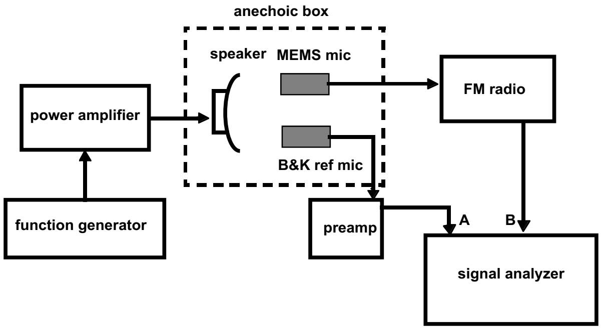

Figure 3: Schematic of experimental setup.

The frequency response of the MEMS microphone was measured by driving the test chamber's built-in loudspeaker and comparing the signals from the MEMS

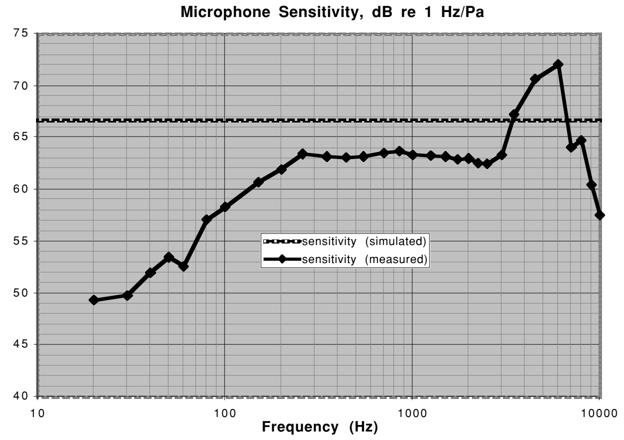

Figure 4: Frequency response of the CMOS-MEMS microphone, measured and predicted.

microphone and the reference microphone. The function generator (Agilent 33120A) was manually stepped through the frequency range of interest, and data points were read from the HP 3562A dynamic signal analyzer. No automation was attempted, because the frequency of the microphone oscillator (around 95 MHz after warming up) drifted slowly with time and so it was necessary to manually tune the radio between data points. Figure 4 shows the output of the microphone in response to the loudspeaker being driven from 20 Hz to 10 kHz. The frequency to volts factor of the radio was measured to be 10 μV/Hz, and a standard FM radio pre-emphasis curve was applied [8].

The noise level of the microphone was measured by repeating the above experiment without driving the loudspeaker. Figure 5 shows the equivalent input noise power density of the MEMS microphone, unweighted, and also A-weighted (A-weighting is a standard function that takes into account the frequency response of the human ear [9]). The A-weighted equivalent noise level of the MEMS microphone is 46 dB SPL. Increasing the number of diaphragms should increase the total capacitance change and reduce the total noise accordingly.

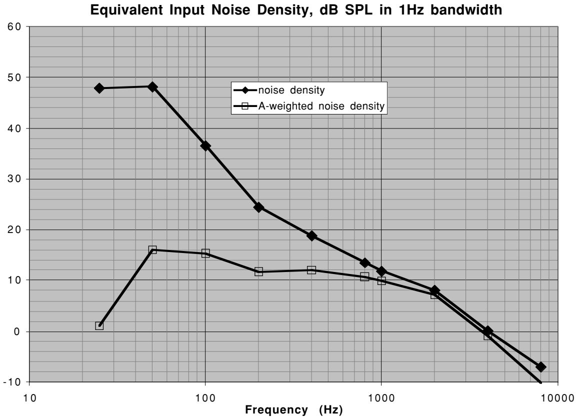

Figure 5: Equivalent input noise density spectrum of MEMS microphone.

The frequency response of the microphone was measured before and after exposure of the microphone to various temperatures (Figure 6). This is an important issue for commercially viable microphones, as the commonly used electret microphones lose their charge and ability to function after exposure to high temperatures, e.g. sitting on a hot dashboard. Because the CMOS-MEMS microphone does not use electret to polarize the capacitor, this is not an issue. However, we want to make sure that the mechanical properties of the sealing polymer are not significantly affected.

For all but one measurement, the packaged chip was placed in a room temperature (20 °C) oven, and the temperature was gradually increased over 30 minutes until the temperature noted on the graph was reached. Then the heating element was turned off and the oven was allowed to cool slowly (another 30 minutes) down to room temperature. The chip was taken out of the oven and the frequency response was measured. The chip was raised to a number of peak temperatures in this manner. Finally, the oven was pre-heated to 250 °C, and the packaged chip was placed in for 7 minutes, and then cooled by setting it out in the room temperature air. The measured change in frequency response relative to the unheated microphone is shown in Figure 6.

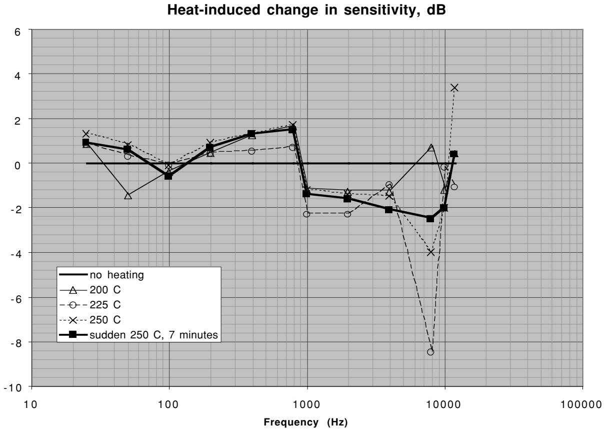

Figure 6: Effect of heating on microphone frequency response.

RESULTS AND CONCLUSIONS

Figure 4 shows the measured frequency response of the microphone. The passband sensitivity is about 5 dB less than predicted, and there is a resonance around 6 kHz, which was predicted to fall above 10 kHz. These indicate that there are inaccuracies in the model. The material properties of the membrane polymer have the greatest uncertainty because of the way in which they were inferred from measurements of previously constructed microspeakers [1]. The sources of uncertainty include neglecting the curvature of the membranes in the microspeakers, tensile stress, and the precise shape of the electric fields between the mesh beams and the silicon substrate (effective capacitance). Most importantly, in the previous work the only clear resonance peaks were from the packaging, making it difficult to determine a precise resonance frequency. New experiments are being performed to more directly measure the material properties based on voltage-deflection measurements. The other notable feature is the drop-of at low frequencies. We believe this is due to leaks in the packaging or microscopic leaks in the membranes. Further investigation is needed.

The unweighted noise density shown in Figure 5 shows a large contribution at low frequencies. This is exaggerated because of the correction for the low sensitivity at low frequencies, but the raw output noise voltage spectrum still has a 1/*f* shape, indicating the source of the noise is electronic rather than thermomechanical. In any case the measured noise was far above the thermomechanical limit. Possible sources of electronic noise in our device include 1/*f* noise from the transistors, Johnson noise, and sensitivity to the power supply voltage (the oscillator frequency was observed to be proportional to the power supply voltage). An Agilent E3631A power supply with heavy RC filtering was used to power the device at 5 volts.

The behavior of the frequency response with respect to temperature changes is encouraging. After a slight (within 2 dB over most of the range) change with bringing the chip up to 200 °C, it appears that raising the temperature further has no systematic effect. This suggests an initial "heat curing" process would guarantee repeatable performance through future heating cycles.

It appears that with some work the performance of a CMOS-MEMS microphone could reach a level sufficient for cell phones, hearing aids and other applications. Obvious improvements include covering a larger area with membranes (to increase capacitance) and develop low-noise circuitry that does not depend on frequency modulation. The limits of performance appear to be related to the quality of the circuit design rather than physical limits of the technology.

AKNOWLEDGEMENTS

This work was supported by DARPA through the MARCO, ICESCATE, and ASIMPS projects.

REFERENCES

[1] J.J. Neumann Jr. and K.J. Gabriel, " CMOS-MEMS membrane for audio-frequency acoustic actuation," *Sensors and Actuators A 95 (2002) 175-182*.

[2] M. Pedersen, W. Olthuis and P. Bergveld, "An Integrated silicon capacitive microphone with frequency-modulated digital output," *Sensors and Actuators A 6 9 (1998) 267-275*.

[3] M. Brauer, A Dehe, T. Bever, S. Barzen, S. Schmitt, M. Fuldner and R. Aigner, "Silicon microphone based on surface and bulk micromachining," *J. Micromech. Microeng.* **11** (2001) 319-322.

[4] Y.B. Ning, A.W. Mitchell, R.N. Tait, "Fabrication of a silicon micromachined capacitive microphone using a dry-etch process," *Sensors and Actuators A 53 (1996) 237-242*.

[5] F.J.M. van der Eerden, H-E.de Bree, H. Tijdeman, "Experiments with a new acoustic particle velocity sensor in an impedance tube," *Sensors and Actuators A 69 (1998) 126-133*.

[6] G.K. Fedder, S. Santhanam, M.L. Reed, S.C. Eagle, D.F. Guillou, M.S.-C. Lu and L.R. Carley, “Laminated High-Aspect-Ratio Microstructures in a Conventional CMOS Process,” *Sensors and Actuators A 57 (1996) 103-110*.

[7] Audio Engineering Society, "Microphones" Anthology, 1979. H.T. Souther, "An Adventure in Microphone Design"; B.B. Bauer, "Equivalent Circuit Analysis of Mechano-Acoustic Structures".

[8] http://www.fmsystems-inc.com/eng_desp.htm (discussion and table of pre-emphasis curve).

[9] F.A. Everest, "Master Handbook of Acoustics", Fourth edition, McGraw Hill, 2001; also, ANSI S1 .4-1971.